Pd nanoparticles formation inside porous polymeric scaffolds followed by *in situ* XANES/SAXS

A Longo[*,1,2], C Lamberti[*,3,4], G Agostini[5,6], E Borfecchia[5], A Lazzarini[5], W Liu[5,7], F Giannici[8], G Portale[1], E Groppo[5]

[1]Netherlands Organization for Scientific Research at ESRF, Grenoble (France); [2]CNR, Istituto per lo Studio dei Materiali Nanostrutturati, Palermo (Italy); [3]Southern Federal University, Rostov-on-Don (Russia); [4]Dept. of Chemistry, CrisDi Centre for Crystallography, University of Turin, Turin (Italy); [5]Dept. of Chemistry, NIS and INSTM Reference Centers, University of Turin, Turin (Italy); [6]European Synchrotron Radiation Facility (ESRF), Grenoble (France); [7]School of Environmental and Chemical Engineering Tianjin Polytechnic University, Tianjin (People's Republic of China); [8]Dipartimento di Fisica e Chimica Università di Palermo (Italy).

E-mail: alessandro.longo@esrf.fr; carlo.lamberti@unito.it

Abstract. Simultaneous time-resolved SAXS and XANES techniques were employed to follow *in situ* the formation of Pd nanoparticles from palladium acetate precursor in two porous polymeric supports: polystyrene (PS) and poly(4-vinyl-pyridine) (P4VP). In this study we have investigated the effect of the use of different reducing agents (H_2 and CO) from the gas phase. These results, in conjunction with data obtained by diffuse reflectance IR (DRIFT) spectroscopy and TEM measurements, allowed us to unravel the different roles played by gaseous H_2 and CO in the formation of the Pd nanoparticles for both PS and P4VP hosting scaffolds.

1. Introduction

In recent years, Pd nanoparticles (NPs) supported on porous polymers have become a promising class of catalysts because of their unique physical−chemical properties and attractive catalytic performances [1]. The polymer acts simultaneously as support and stabilizer, thanks to the dual effect of porosity (steric stabilization) and charged functional groups (electrostatic stabilization) [2,3]. For this reason, Pd catalysts supported on polymers are more stable than the homogeneous counterparts; moreover, they are cheaper, easy to handle, and easily recovered. XAFS techniques have been largely employed to characterize metal NPs [4,5], sometimes in combination with other techniques such as XRPD, IR, and SAXS [6]. In this contribution we present a simultaneous XANES/SAXS study, performed on the BM26A beamline of the ESRF [7], to follow *in situ* the formation of Pd nanoparticles in PS and P4VP porous polymers. Parallel laboratory IR and TEM study complement the XANES/SAXS investigation.

2. Experimental

The starting Pd(II)−polymer composite was prepared by impregnation, stirring the highly cross-linked polymers polymer (both a poly(4-ethylstyrene-co-divinylbenzene), hereafter PS and a poly(4-vinylpyridine-co-divinylbenzene), hereafter P4VP from Aldrich) with an appropriate amount of palladium acetate in acetonitrile, resulting in a final Pd loading of 10 wt % [8,9]. *In situ* reduction of

the Pd(II)−polymer to get Pd(0)-containing polymer was carried out in mild conditions in flow of H_2 or CO reducing agents in the gas phase (both diluted at 5% in He).
FT-IR spectra were collected in reflectance mode (DRIFT) on a Nicolet 6700 instrument, equipped with a MCT detector. A Thermo Fisher Environmental Chamber was adopted to record FT-IR spectra in reaction conditions. Transmission electron micrographs were obtained using a JEOL 3010-UHR instrument operating at 300 kV, equipped with a 2k × 2k pixel Gatan US1000 CCD camera.
The SAXS/XAS set up used at BM26A @ ESRF was described elsewhere [7]. The energy delivered by the double crystal Si(111) monochromator was calibrated measuring the XANES spectrum of a Pd foil in transmission mode. Fluorescence XANES spectra at the Pd K-edge (24.3 keV) were collected with a nine-element Ge detector. The SAXS patterns were collected using a 2D Mar detector. The sample−detector distance was calibrated with standard Ag behenate. The energy change between the start and the end of the XANES spectrum (about 120 eV) is irrelevant to SAXS at that high energy, so the incident beam wavelength can be treated as constant, $\lambda = 0.509(1)$ Å. The resulting q-range was 0.5−7.0 nm^{-1} ($q = 4\pi \sin(\theta)/\lambda$, where θ is the X-ray scattering angle), allowing investigation of the 12.5−0.9 nm d-spacing interval. Each XANES spectrum was collected in about 300 s. As the readout and erasing time of the 2D Mar detector was 180 s, each SAXS pattern was collected for 120 s resulting in a 1 to 1 correspondence between XANES spectra and SAXS patterns.

3. Results and discussion

A summary of the data and of the analysed results is reported in Figures 1 and 2. We have demonstrated that the nature of the polymeric matrix has a strong influence on the formation of the Pd NPs and affects their final properties, in terms of particle size, electronic properties, and type and fraction of accessible surface sites. In particular, the presence of nitrogen-based ligands allows the formation of extremely small, subnanometric Pd clusters in P4VP, as demonstrated by the observation of a specific interaction between Pd nanoparticles and the nitrogen of the pyridine ligands [8]. For both Pd/PS and Pd/P4VP systems, the reduction process is strongly dependent on the nature of the reduction agent (H_2 or CO) [9].
For the Pd/PS systems the following conclusions have been obtained: (i) Reduction of palladium acetate starts at lower temperature (already at room temperature) and proceeds faster in the presence of CO than with H_2. (ii) The Pd NPs are bigger when formed in CO and show peculiar morphologies (triangles and hexagons, see inset in Figure 1a), whereas those formed in H_2 are smaller and spherical in shape (Figure 2b). (iii) Pd NPs formed in CO have unclean surfaces, probably as a consequence of residual by-products (such as acetic anhydride) that are not desorbed at the reduction temperature, as evidenced by DRIFT [9]. The reason for the different properties of the formed Pd NPs has to be related to the different mechanism of palladium acetate reduction. It is likely that, in the presence of CO, Pd acetate carbonyl intermediates are formed, where CO acts as templating agent, promoting the crystal growth in specific directions. This is relevant as the catalytic reactivity of metal NPs depends not only on the size (and size distribution) control but also on the exposure of the peculiar (hkl) planes.
For the Pd/P4VP system (Figure 2f-l), we have demonstrated that the presence of the basic pyridine functional groups inside P4VP facilitates the dispersion of palladium acetate in a monomeric form, in which the acetate ligands assume a mono-dentate configuration [8,9]. This peculiar structure of Pd-acetate in P4VP is at the basis of its different reactivity towards reducing agents with respect to the observations made for Pd/PS, where functional groups are absent. In particular, H_2 efficiently reduces palladium acetate in P4VP, to give palladium nanoparticles and acetic acid. The latter is stabilized by the basic functional groups in the polymer, which make possible its spectroscopic observation. The consequence is that reduction occurs at a higher temperature than for palladium acetate dispersed in PS (that has no functional groups), as determined by DRIFT and XANES spectroscopy. In addition, the Pd NPs are smaller (as determined by TEM and SAXS), as they are stabilized by direct covalent interaction with the nitrogen-containing ligands, in good agreement with previous findings [8]. On the contrary, CO does not reduce palladium acetate (data not shown). Isolated Pd^{2+} carbonyl adducts are immediately formed, with the simultaneous displacement of the acetate ligands, as detected by DRIFT

spectroscopy. These Pd^{2+} carbonyl adducts easily migrate and aggregate in units of about 5 nm that, having a higher electronic density with respect to the hosting matrix, are easily revealed by SAXS.

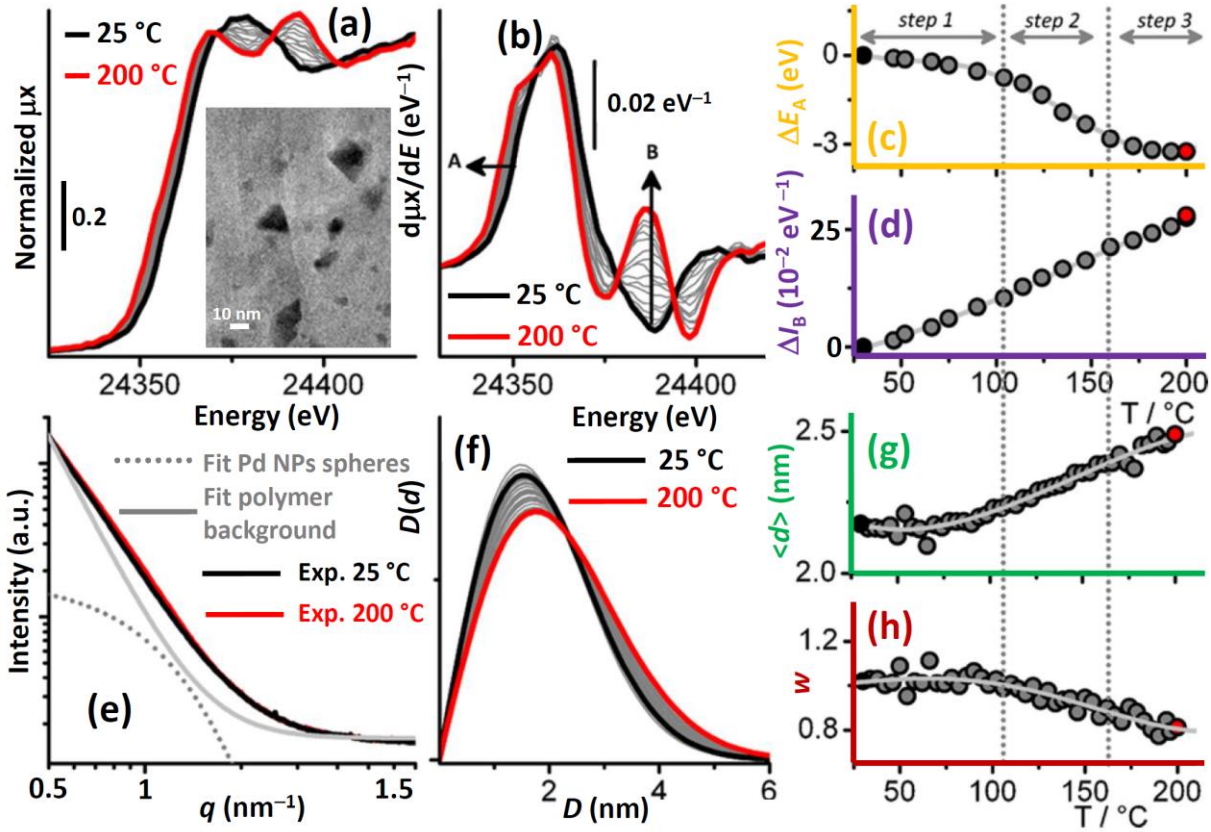

Figure 1. SAXS−XAS data collected simultaneously during reduction of Pd/PS in CO/He flow from 25 °C (black) to 200 °C (red); heating rate 2 °C/min. Parts (a, b): evolution of the normalized XANES spectra and of the derivative signal. Parts (c, d): evolution as a function of temperature of features A (shift in energy) and B (change in intensity) of the derivative XANES spectra, see arrows in part (b). Part (e): SAXS pattern at the beginning (black) and the end (red) of the temperature ramp. Also examples of the theoretical signals obtained by considering a distribution of spherical particles (dotted gray) and the background (gray) are reported. Part (f): evolution of the particle size distribution as a function of the temperature. Parts (g,h): average diameter of the Pd particles and relative weight as a function of temperature, respectively, as obtained from the spherical model fitting of the Pd NPs contribution to the SAXS data. The inset in part (a) reports a representative TEM micrograph of the CO-reduced Pd/PS system. Adapted with permission from Ref. [9a], copyright American Chemical Society 2014.

4. Conclusions and acknowledgements

These findings have important potential implications in the field of catalysis. For example, it is expected that reactions catalyzed by palladium acetate and involving carbon monoxide would have a different outcome when palladium acetate is hosted in porous P4VP than in other supports without pores and/or nitrogen containing ligands. Finally, the importance of a multi-technique approach in following the whole process of metal nanoparticles formation clearly emerges.

We are grateful to R Pellegrini (Chimet SpA) and G Leofanti for constructive discussions. C. L. acknowledges the megagrant of the Russian Federation Government to support scientific research at the Southern Federal University, no. 14.Y26.31.0001.

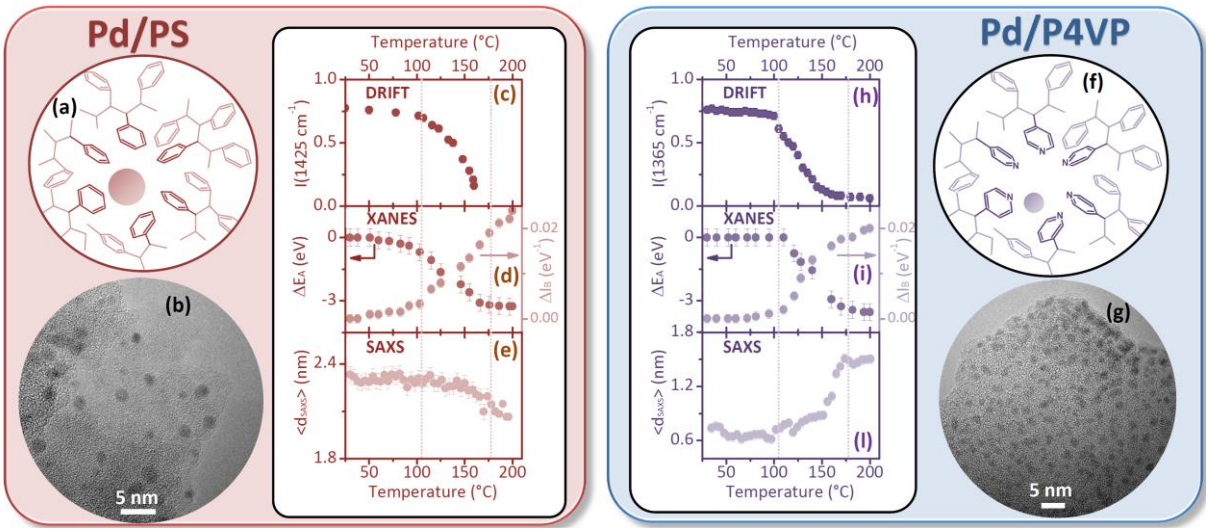

Figure 2. Part (a): cartoon representing a Pd NPs hosted inside PS matrix. Part (b) representative TEM micrographs of the H_2-reduced Pd/PS system. Parts (c-e): Summary of the DRIFT and of the SAXS−XAS data collected simultaneously during reduction of Pd/PS in H_2/He flow. Evolution as a function of temperature of: part (c) the intensity of the IR absorption band, which is characteristic of the acetate ligand [9]; part (d) features A (shift in energy, left axis) and B (change in intensity, right axis) of the derivative XANES spectra (as marked in Figure 1b) and part (e) average Pd particle size as obtained from analysis of the SAXS data (same approach as shown in Figure 1e. (f-l): as parts (a-e) for the DRIFT and the SAXS−XAS data collected simultaneously during reduction of Pd/P4VP in H_2/He flow. Previously unpublished figure comparing data discussed in Refs. [9a] and [9b].

References

[1] (a) Hodge P 1997 *Chem. Soc. Rev*. **26** 417; (b) Akiyama R and Kobayashi, S 2009 *Chem. Rev*. **109** 594
[2] Roucoux A Schulz, J and Patin H 2002 *Chem. Rev*. **102** 3757
[3] Ott L S and Finke R G 2007 *Coord. Chem. Rev*. **251** 1075
[4] (a) Newton M A 2008 *Chem. Soc. Rev*. **37** 2644; (b) Frenkel A I 2012 *Chem. Soc. Rev*. **41** 8163
[5] (a) Bordiga S, Groppo E, Agostini G, van Bokhoven J A and Lamberti C. 2013 *Chem. Rev*. **113** 1736; (b) Mino L, Agostini G, Borfecchia E, Gianolio D, Piovano A, Gallo E and Lamberti C. 2013 *J. Phys. D: Appl. Phys*. **46** 423001; (c) Garino C, Borfecchia E, Gobetto R, van Bokhoven J A, Lamberti C. 2014 *Coord. Chem. Rev*. **277–278** 130.
[6] (a) Lamberti C, Borfecchia E, van Bokhoven J A, and Fernández García M 2016 in *X-Ray Absorption and X-ray Emission Spectroscopy: Theory and Applications*, Eds. van Bokhoven J A, and Lamberti C, Chapter. 12, Vol. 1 (Chichester: John Wiley & Sons) p 303; (b) Groppo E, Agostini G, Piovano A, Muddada NB, Leofanti G, Pellegrini R, Portale G, Longo A, Lamberti C 2012 *J. Catal*, **287** 44; (c) Agostini G, Lamberti C, Pellegrini R, Leofanti G, Giannici F, Longo A, Groppo E, 2014 *ACS Catal.* **4**, 187
[7] (a) Longo A, Portale G, Bras W, Giannici F, Ruggirello A M and Turco Liveri V 2007 *Langmuir* **23** 11482; (b) Nikitenko S, Beale A M, van der Eerden A M J, Jacques S D M, Leynaud O, O'Brien M G, Detollenaere D, Kaptein R, Weckhuysen B M, and Bras W 2008 *J. Synchrotron Radiat*. **15** 632
[8] Groppo E, Liu W, Zavorotynska O, Agostini G, Spoto G, Bordiga S, Lamberti C and Zecchina A, 2010 *Chem. Mater*. **22** 2297
[9] (a) Groppo E, Agostini G, Borfecchia E, W Liu, Giannici F, Portale G, Longo A and Lamberti C, 2014 *J. Phys. Chem. C*, **118** 8406; (b) Groppo E, Agostini G, Borfecchia E, Lazzarini A, W Liu, Lamberti C, Giannici F, Portale G and Longo A 2015 *ChemCatChem*, **7** 2188